A Comprehensive Database of Leaf Temperature, Water, and CO 2 Fluxes in Young Oil Palm Plants Across Diverse Climate Scenarios

Raphael Perez, Valentin Torrelli, Sandrine Roques, Sébastien Devidal, Clément Piel, Damien Landais, Merlin Ramel, Thomas Arsouze, Julien Lamour, Jean-Pierre Caliman, et al.

A Comprehensive Database of Leaf Temperature, Water, and CO_2 Fluxes in Young Oil Palm Plants Across Diverse Climate Scenarios

Raphael Perez[1,2], Valentin Torrelli[1,2,3,4], Sandrine Roques[1,2], Sébastien Devidal[5], Clément Piel[5], Damien Landais[5], Merlin Ramel[3,4], Thomas Arsouze[3,4], Julien Lamour[6], Jean-Pierre Caliman[7], Rémi Vezy[3,4]

[1]*CIRAD, UMR AGAP Institut, F-34398 Montpellier, France*
[2]*UMR AGAP Institut, Univ Montpellier, CIRAD, INRAE, Institut Agro, F-34398 Montpellier, France*
[3]*CIRAD, UMR AMAP, F-34398 Montpellier, France 4*
[4]*AMAP, Univ. Montpellier, CIRAD, CNRS, INRAE, IRD, F-34398 Montpellier, France*
[5]*Ecotron Européen de Montpellier, Unité Propre de Service 3248, Centre National de la Recherche Scientifique (CNRS), Campus Baillarguet, F-34980 Montferrier-sur-Lez, France;*
[6] *Centre de Recherche sur la Biodiversité et l'Environnement (CRBE), Université de Toulouse, CNRS, IRD, Toulouse INP, Université Toulouse 3 – Paul Sabatier (UT3), Toulouse, France.*
[7]*SMART Research Institute, Pekanbaru 28112, Indonesia*

Abstract

Functional-structural plant models (FSPM) aim to replicate the intricate ecophysiological and developmental responses of plants to their environment. These models are valuable for projecting plant behaviour in a changing climate but rely heavily on detailed measurements of structural and ecophysiological traits for their parameterization. However, collecting these measurements simultaneously and consistently at multiple scales remains a challenge, often limiting model parameterization and thorough evaluation, and thereby reducing confidence in model predictions.

Here, we propose a comprehensive dataset of biophysical measurements from four oil palm plants grown (*Elaeis guinnensis)* in controlled environments. The dataset includes detailed reconstructions of the three-dimensional plant structures derived from terrestrial LiDAR point clouds and leaf-scale gas exchange measurements for parameterising leaf physiology. We also provide plant-scale gas exchange measurements (CO_2 and H_20) and leaf temperature data under multiple controlled environmental scenarios, including varying CO_2 concentrations, light, temperature and humidity conditions. Our aim is to create a digital twin of the four plants to facilitate FSPM robust evaluation, and help identify sources of model uncertainty.

Keywords: response curve; FSPM; temperature; radiation; VPD; CO_2

Introduction

Biophysical plant models aim to mechanistically represent how plants acquire, process, and utilise biophysical resources—such as light, water, and carbon—across spatial and temporal scales by integrating fundamental physiological processes such as photosynthesis, transpiration or energy balance. These models are used by different communities of scientists interested in the simulation of plants at different scales: organ-to-plant with functional-structural plant models (Vos et al., 2010), plant-to-plot with individual process-based models (*e.g.* Duursma and Medlyn, 2012 or Maréchaux and Chave, 2017), or earth models (*e.g.* Krinner et al., 2005).

Generally, these models use leaf-scale measurements to parameterise different sub-models, enabling the upscaling of such measurements to the plant or plot level, thereby simulating variables that are hard or impossible to directly measure (*e.g.* water and energy balance) and predicting system behaviour under current or new conditions (*e.g.* assessing climate change impacts). Evaluating a model becomes more challenging when numerous interconnected processes are simulated, as is often the case with biophysical processes in natural systems, and these interactions may act across different scales. Yet, despite their broad relevance, these models are often evaluated using data collected at a single scale—most commonly at the leaf or plot level—due to the rarity of datasets that capture both detailed organ-level measurements and integrated responses at the whole-plant scale. In practice, the challenge of acquiring coherent datasets that simultaneously capture plant geometry, physiological traits, and whole-plant gas exchange under controlled and well-documented conditions often restricts the thorough assessment of models. Consequently, most models remain untested or insufficiently evaluated at integrative levels, reducing our confidence in their predictions and their applicability to real-world scenarios.

We argue that accessible databases allowing to evaluate biophysical models at different scales, from the leaf to the plant and plot are crucial for increasing confidence in model predictions. Those databases should include different experiments conducted in more to less controlled conditions, allowing the evaluation of models with more or less degrees of freedom, evaluating physics-based processes first, and coming to more biology-based processes. For example, the experimental data acquired by Schymanski and Or (2017) can help evaluate the energy balance (sensible and latent heat) components of models at the scale of an individual leaf, thanks to their experiment on highly controlled conditions using an artificial leaf.

In this paper, we address the following critical gap by providing a comprehensive database of biophysical measurements in young oil palm plants (*Elaeis guineensis*) to evaluate

biophysical processes at leaf-to-plant scale under controlled conditions. Our dataset encompasses detailed 3D reconstructions of plant structure, leaf-level gas exchange measurements that inform fundamental physiological parameters, and concurrent whole-plant flux data acquired under controlled dynamically varying climatic conditions. By bridging the scales from individual leaves to the entire plant, this database allows modellers to both calibrate their biophysical models at a fine spatial resolution and evaluate their predictive accuracy at a more holistic level: the whole plant. In doing so, we take a crucial step toward a new generation of open-access databases that empower researchers to rigorously benchmark biophysical models, ultimately improving their robustness, reliability, and utility.

Plant material and pre-experiment growing conditions

Four oil palm plants (*Elaeis guineensis Jacq.*) from two genetic origins were studied: Deli x Lame crossing (P1, P2 & P4) and a Deli x Yamgambi crossing (P3). The plants were sown on May 11th 2020 and cultivated in a greenhouse from CIRAD's Abiophen platform (Montpellier, France). The air temperature was controlled at 26°C during the day and 21°C during the night, relative humidity at 70%, photosynthetically active radiation (PAR) at 600 µmol m^{-2} s^{-1}, and air CO_2 concentration ([CO_2]) at around 400 ppm. The plants were irrigated every two to three days to prevent water stress. On February 25th 2021, the plants were transferred to the microcosm's experimental platform of the European Ecotron of Montpellier (https://www.ecotron.cnrs.fr).

Microcosms

Set-up

Two microcosms growth chambers of dimensions 114 cm width x 113 cm depth x 152 cm (~1.5 m^3) height were used for the two-month experiment. The microcosms allowed for a precise control of radiation in the visible spectrum (PAR) with four LED lamps, air temperature (5-50±0.5°C), relative humidity (20-90±3%), and CO_2 concentration (10-2000ppm). The monitoring microcosm was used to measure the biophysical processes of a single plant in response to different climate conditions with varying air temperature, relative humidity and radiation. The storage microcosm was used to store the three other plants waiting for their turn in the monitoring microcosm.

Monitoring

The monitoring microcosm was operated as an open CO_2 gas exchange system. The flow rate of dry air at the inlet was measured and regulated at 4.9 Nm^3 h^{-1} using a mass flow regulator (F-202AV, Bronkhorst, The Netherlands). The net CO_2 flux was measured continuously by sequentially measuring the inlet and outlet of the chamber every 5 minutes

using a Valco selector (EUTA-SD4MWE, VICI, Switzerland) and a Picarro G2101-i (Picarro, USA) CO_2 analyser. For each position of the selector, the first two minutes were discarded, and the last three minutes were averaged. The air sampling at the inlet circulated first through a 30-litre buffer volume with a flow rate regulated at 1.5 l min^{-1} using a needle valve, while the outlet was directly measured.

The monitoring microcosm was also equipped with a photosynthetically active radiation sensor (PAR, Figure 1), air temperature and humidity sensors, a thermal camera on the top left corner pointing towards the centre of the chamber to measure leaf temperature, and a precision scale to monitor weight. The thermal camera and the precision scale were controlled by a Raspberry Pi (https://www.raspberrypi.org/) board that triggered a camera shot every minute and automatically logged the stream of data from the scale. Data from all other sensors were automatically logged by the microcosm facility.

The pot of the plant was sealed before entrance into the monitoring microcosm to avoid water loss to the atmosphere, enabling the computation of plant transpiration from weight loss. Plants were automatically watered every six hours to maintain non-limiting soil water availability.

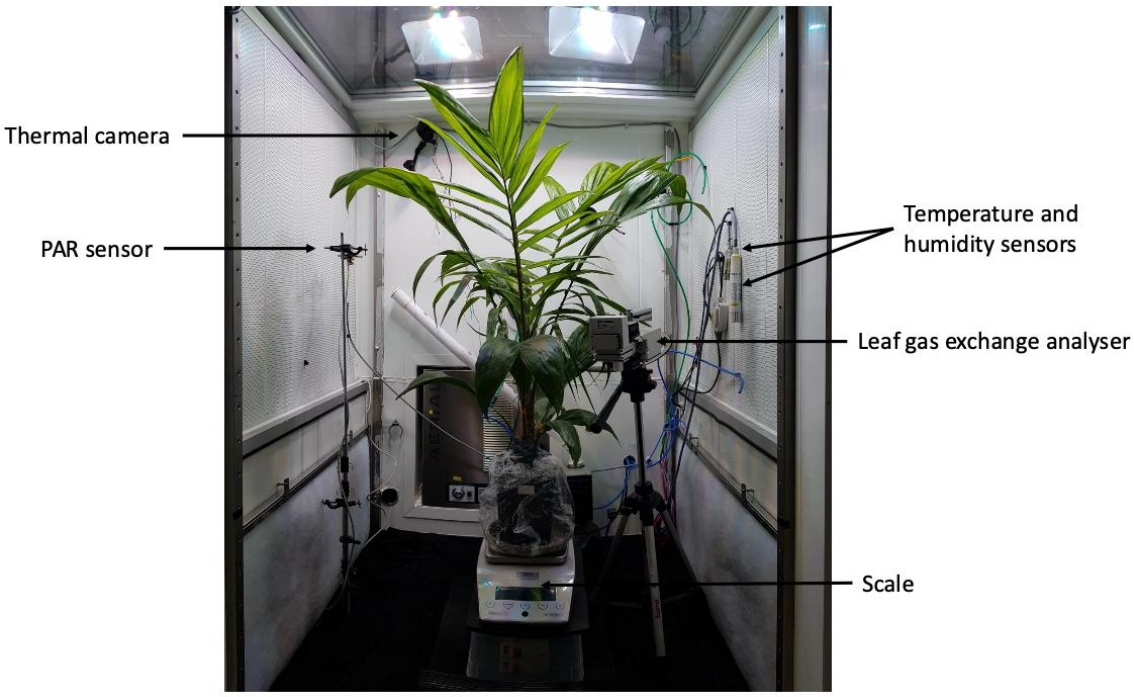

Figure 1: Oil palm plant in the monitoring microcosm. The pot was sealed to avoid water loss to the atmosphere. A precision scale was positioned under the pot to estimate plant transpiration from variations in plant weight. Sensors for photosynthetically active radiation, temperature, and relative humidity were installed in the chamber to regulate the environmental conditions. The head of the leaf gas exchange analyser was positioned in the chamber to conduct either CO_2 response curves in the storage microcosm or to follow leaf assimilation during specific scenarios (WalzOpen or WalzClose tests) in the monitoring chamber.

Plant-level CO_2 and H_2O gas exchanges

The net flux of CO_2 was calculated from the inlet and outlet fluxes following (Eq1):

$$N = D(C_{in} - C_{out}) \qquad \text{(Eq1)}$$

Where N is the net flux of CO_2, in µmol s^{-1}, D is the flow rate of air at the inlet of the chamber, in µmol s^{-1}, C_{in} and C_{out} are the mixing ratio of CO_2 corrected for dilution by water vapour, respectively at the inlet and outlet of the chamber, in µmol mol^{-1}.

Because the pot of the plant was sealed, any variation in the weight measured from the scale could be attributed to plant transpiration. Large increases in pot weight were used as indicators of irrigation. Transpiration was then estimated using two different methods. The first method measured the difference in pot weight between the start and end of a specified time interval. The second, known as the regression method, determined transpiration by calculating the slope of a linear regression fitted to all weight measurements within that interval.

Scenarios

The climate conditions in the microcosm were defined based on the average daily variation observed at a weather station in Pekanbaru, Indonesia, where the conditions are optimal for oil palm cultivation. The *base conditions* consisted of a constant [CO_2] at 400 ppm, daily fluctuations of air temperature from 22°C to 33°C, relative humidity from 82% to 51%, and PAR from 0 to approximately 300 µmol m^{-2} s^{-1} at mid-height within the chamber and ~1000 µmol m^{-2} s^{-1} below the light source. The climate conditions were fixed to the base conditions in the storage microcosm for the whole duration of the experiment.

Varying daily conditions were simulated based on the *base conditions* by adjusting the CO_2 concentration, radiation, temperature, and relative humidity. The resulting climate scenarios were as follows (Figure 2):

- “400 ppm”: base conditions
- “600 ppm”: base conditions with 600 ppm [CO_2];
- “800 ppm”: base conditions with 800 ppm [CO_2];
- “Cloudy”: base conditions with decreased PAR radiation, set to 130 µmol m^2 s^{-1} at mid-day and mid-height within the chamber;
- “Cold”: base conditions with -30% °C;
- “Hot”: base conditions with +30% °C;
- “DryCold”: base conditions with +30% of relative humidity and -30% °C;

- “DryHot”: base conditions with -30% of relative humidity and +30% °C;

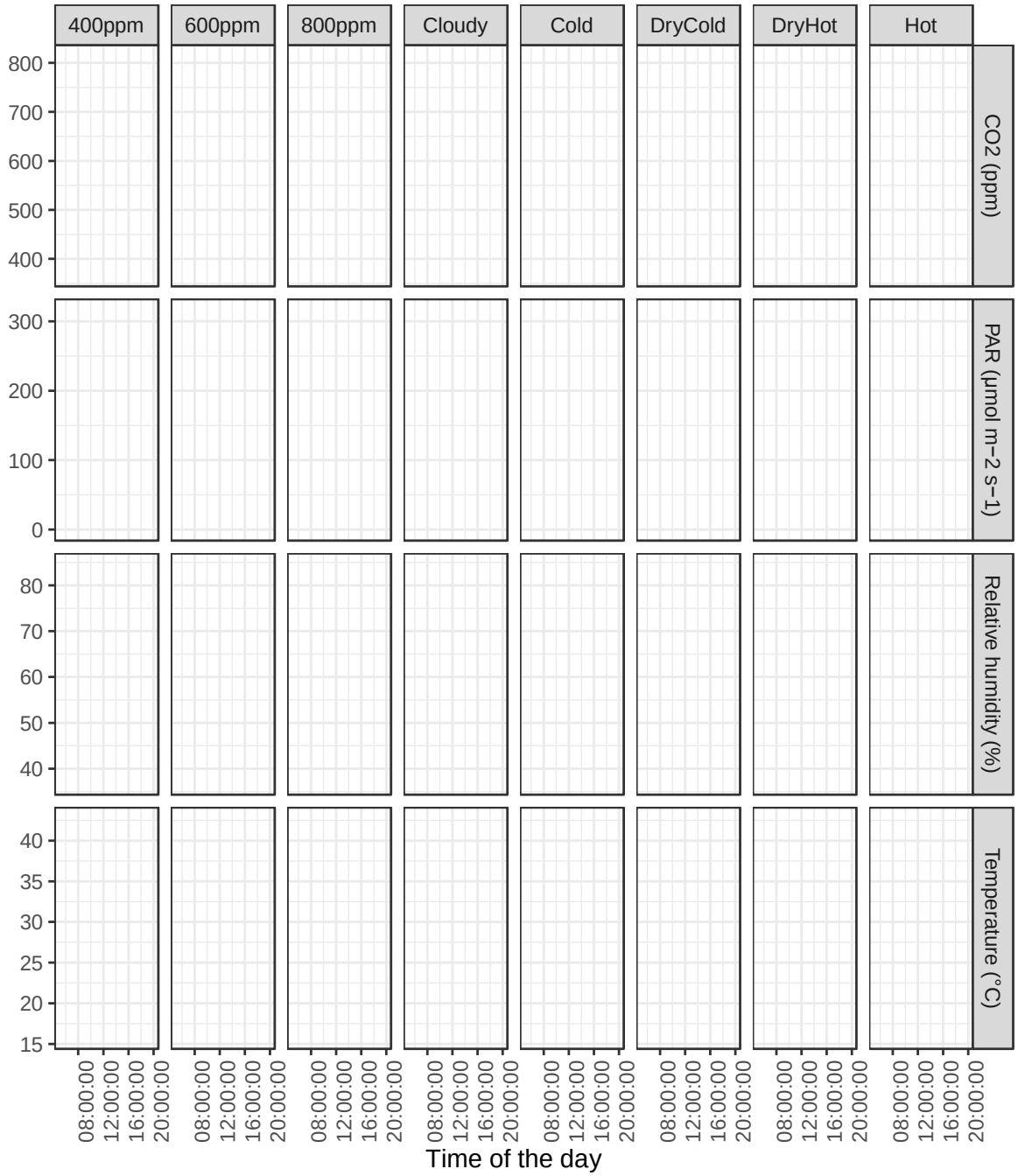

Figure 2: Monitoring radiation, air temperature, and relative humidity over time for the eight climate scenarios. Each transparent line represents a day of measurement. Photosynthetically active radiation was measured at the chamber's centre height. The reference scenario is the ‘400ppm’ scenario.

Each plant was sequentially placed in the monitoring microcosm for one or several days, resulting in the design of the experiment presented in Figure 3. The scenarios with potential negative impacts on plant function due to extremely high temperatures were performed on each plant's last days of measurements. Some repetitions of scenarios were performed to

estimate changes in plant function over time.

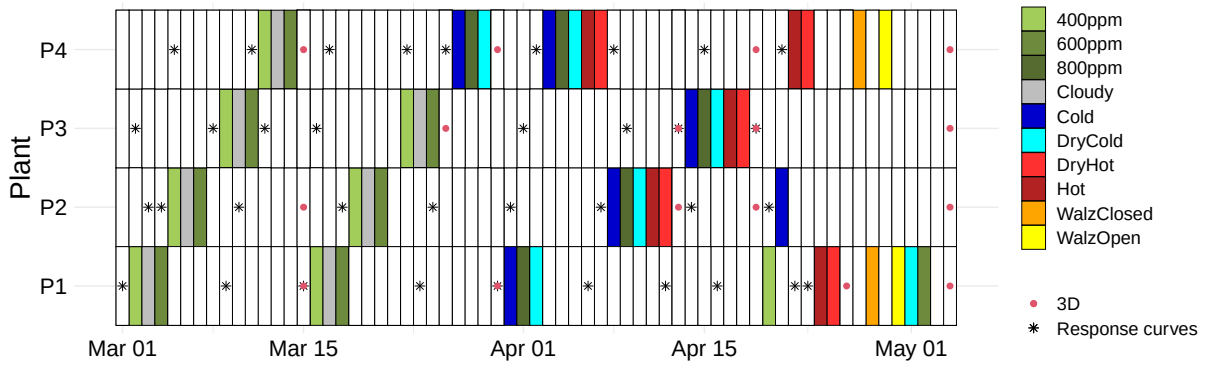

Figure 3: Climate scenarios set in the monitoring microcosm and the sequence of measurements. Grey cells indicate dates on which the plant is in the storage microcosm. Points indicate the date of leaf gas exchange measurement (black crosses) and dates of 3D reconstruction of plants (red points).

Leaf-level CO_2 and H_2O gas exchanges

Leaf gas exchange measurements were performed with a Walz GFS-3000 portable gas analyser with a Walz PAM-Fluorometer 3056-FL and a cuvette area of 8 cm^2. One leaf per plant was regularly measured in the storage microcosm during the experiment (responses curves, Figure 3) before and after the climatic scenarios. At each date, the leaf photosynthesis response to CO_2 ($A{\sim}C_i$ curves) was measured, followed by the photosynthesis response to photosynthetic photon flux density (A~PPFD curves) and stomatal conductance response to vapour pressure deficit (G_s~VPD).

The $A{\sim}C_i$ curves were performed at a saturating PPFD of 1500 µmol m^{-2} s^{-1}, a controlled cuvette air temperature of 25°C, a relative humidity of 65%, a constant air flow rate through the cuvette of 750 mL min^{-1}, and changing [CO_2] from 400 to 50 ppm, then from 400 to 2000 ppm in 13 steps total.

The light curves were performed after an acclimation to ambient CO_2 of 6 minutes after the A-Ci curves. The temperature and relative humidity were maintained the same as for the A-Ci curves and the light was changed in 9 steps from 1500 µmol m^2 s^{-1} of PAR to 10 µmol m^2 s^{-1} of PAR.

The G_s~VPD curves were measured in 7 steps from 0.7 kPa to 2.5 kPa at 1500 µmol m^2 s^{-1} of PAR and 400 ppm [CO_2]. The VPD was controlled by changing the relative humidity (from 75% to 30%) and the air temperature (from 23°C to 27°C).

These response curves can be used to estimate the parameters of coupled leaf photosynthesis and transpiration models (Busch et al., 2024). In the dataset, we used the $A{\sim}C_i$ curves to estimate the Farquhar-von Caemmerer-Berry (FvCB) of C3 photosynthesis (Farquhar et al., 1980) parameters at a reference temperature of 25°C using the temperature-dependent parameters from Kumarathunge et al., (2019), except for the rate of

decrease of the function above the optimum for the rate of electron transport (Hd_j) and rubisco activity (Hd_v) that were taken from Dreyer et al. (2001) and Medlyn et al. (2002). The estimated parameters included the maximum rate of rubisco carboxylation (V_{cmax}), the maximum potential electron transport rate (J_{max}), the rate of mitochondrial respiration (R_d) and the triose phosphate utilisation rate (*TPU*, Figure 4a*)*. Response curves to VPD were used to estimate the parameters of Medlyn's stomatal conductance model (Medlyn et al., 2011), *i.e.* the residual stomatal conductance (g_0) and the slope parameter (g_1, Figure 4b), although other models could be used.

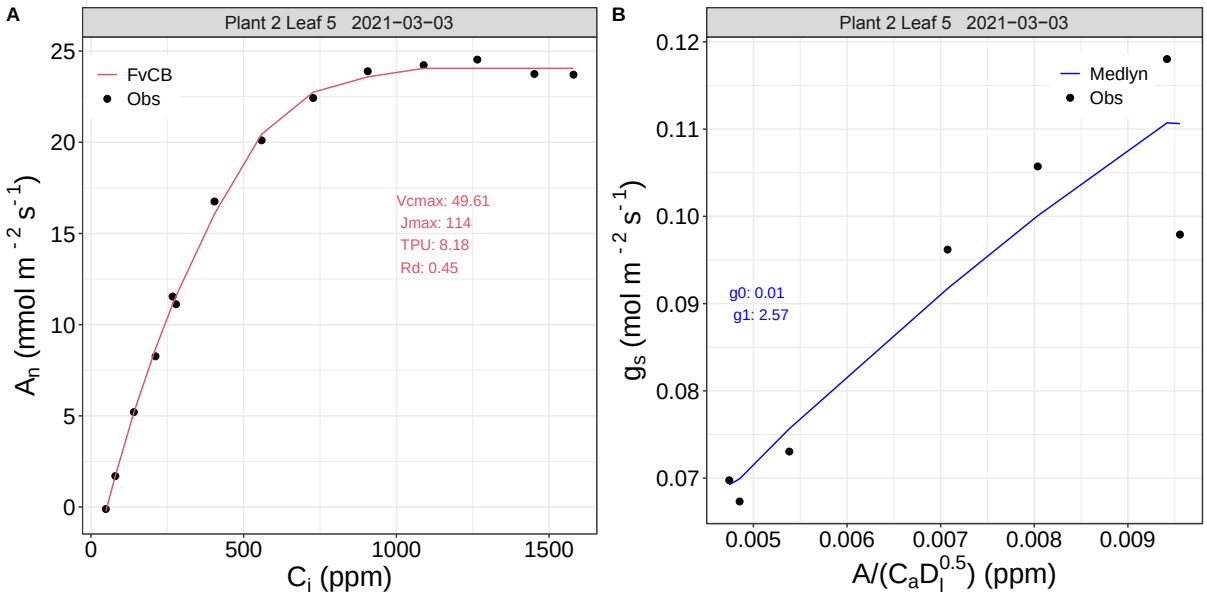

Figure 4: Calibration of photosynthesis and stomatal conductance models from leaf gas exchange responses curves. A) A~C_i response curve fitted with the Farquhar-von Caemmerer-Berry (FvCB) model. B) The G_s~VPD (Dl) response curve is fitted with Medlyn's stomatal conductance model (Medlyn et al., 2011).

The last week of the experiment, additional measurements were conducted on two plants (Figure 3) to assess the correlations between leaf-level gas exchanges and plant-level gas exchanges. The aim was to investigate whether leaf gas exchange is influenced by overall plant conditions, mainly focusing on the light environment. The plant was placed in the flux chamber, with one leaf attached to the Walz leaf gas analyser. The conditions within the Walz's head remained constant in terms of temperature, [CO_2] and relative humidity, while the light was either at saturation (1500 µmol m^{-2} s^{-1}; WalzClosed test) or following the ambient conditions of the microcosm by removing the light component from the head (WalzOpen test). During both tests, the climate conditions within the microcosm followed the reference scenario (400 ppm), but the light ranged from darkness to peak photosynthetically active radiation (PAR) levels (Figure S1).

Leaf temperature

Leaf temperature was measured with a FLIR Vue™ Pro R thermal camera triggered by a Raspberry Pi to take one image every second automatically. The camera was installed on the top left corner of the chamber and oriented toward the centre of the microcosm to ensure optimal coverage of the plant canopy. Images were continuously recorded from March 2nd to May 3rd and later processed to extract regions corresponding to identifiable leaves from each frame. For every image, fixed masks were defined to isolate the maximum consistently visible area of each leaf, accounting for slight movements induced by wind inside the chamber (Figure 5). Leaf temperatures were calculated after adjusting for air temperature and relative humidity within the chamber. Finally, the mean, maximum, minimum and standard deviation of the temperatures within each mask were computed.

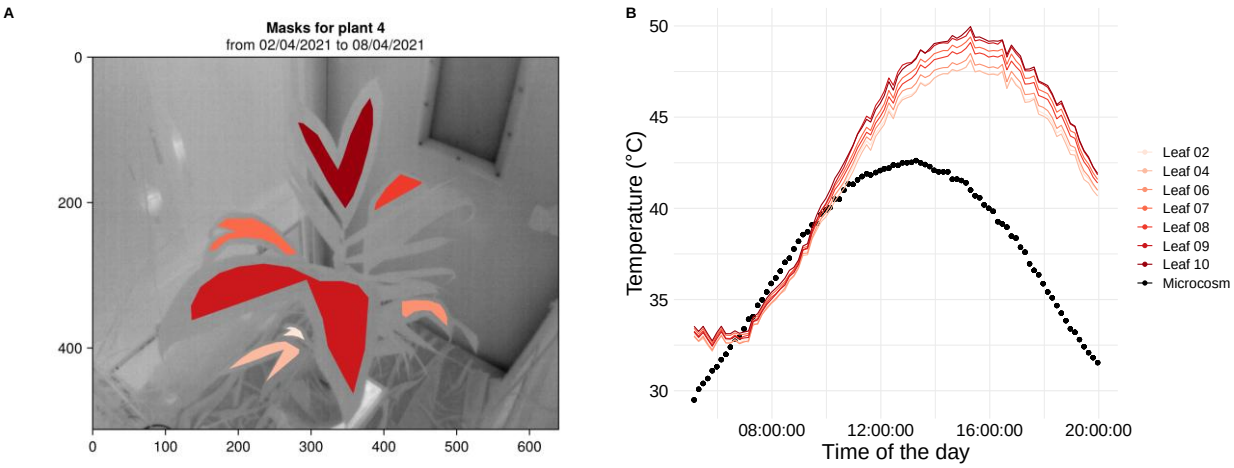

Figure 5: A) Masks of leaf area for estimating leaf temperature. The mask is located at the centre of the leaf to avoid capturing image pixels that may not consistently represent the leaf due to internal chamber wind. The colours represent the different masks of the monitored leaves. B) Temperatures of leaves and the air temperature (black points) over a day.

Leaf chlorophyll content

The chlorophyll content of leaves was measured with a SPAD chlorophyll meter (SPAD-502; Minolta, Ltd., Japan). At the beginning of the experiment (February 16th and 23th), SPAD readings were taken on every leaf of all the plants. Then, SPAD measurements were repeated on all leaves of each plant prior to conducting leaf gas exchange measurements in the microcosm.

Plants architecture

LiDAR scans of the four plants were conducted every week throughout the entire period of flux measurements. At least three viewpoints were captured for the co-registration process to accurately represent the whole plant and minimise occlusion issues. At the end of the experiment, the leaves were removed from the plant and scanned individually, a step that

enabled detailed reconstruction of each leaf for each date—particularly in the densely overlapping central regions—without interference from adjacent foliage.

Plant reconstructions were carried out manually in Blender (Blender Online Community, 2022). Using plane meshes fitted to the leaf point clouds via the *poly build tool* with automatic vertex merging (Figure 6A), each organ was reconstructed separately and exported as a `ply` file.

To overcome the challenge of distinguishing overlapping leaves in the central region, we leveraged the individual leaf reconstructions to guide the plant-scale point clouds reconstructions. Starting with the latest LiDAR scan (which was closest in time to the individual leaf scans), we integrated these detailed leaf models into the overall reconstruction. Then, proceeding chronologically backward, we manually modified and adjusted the meshes to fit the point clouds of preceding dates, using the later reconstructions as references. This sequential, reference-based approach enhanced the consistency and accuracy of the reconstructions over time (Figure 6B).

Figure 6: 3D reconstruction from LiDAR point clouds. A) Building plane meshes on point cloud with the poly build tool of Blender. B) Full reconstruction of the 3D mock-up from points cloud.

Each time a plant was placed in the microcosm to undergo a climate scenario sequence, we selected the LiDAR point cloud that best represented these dates for reconstruction. Due to

the slow development of the plants. Ultimately, four dates were chosen to capture the evolution of the plant architecture for each plant (Figure 3).

In the final step, each ply file was converted into an Open Plant Format (OPF, Griffon and de Coligny, 2014), a portable file that stores both plant topology and geometry and is commonly used in simulation models of biophysical processes. The plant topology was defined by six symbols: Plant, Pot, Bulb, Stipe, Leaf and Spear.

The quality of the virtual reconstructions was assessed by comparing the area of each virtual leaf to measurements obtained with a leaf area meter (Licor LI-3100C) at the end of the experiment. The results demonstrated a high level of agreement between the measured and reconstructed leaf areas (Figure 7).

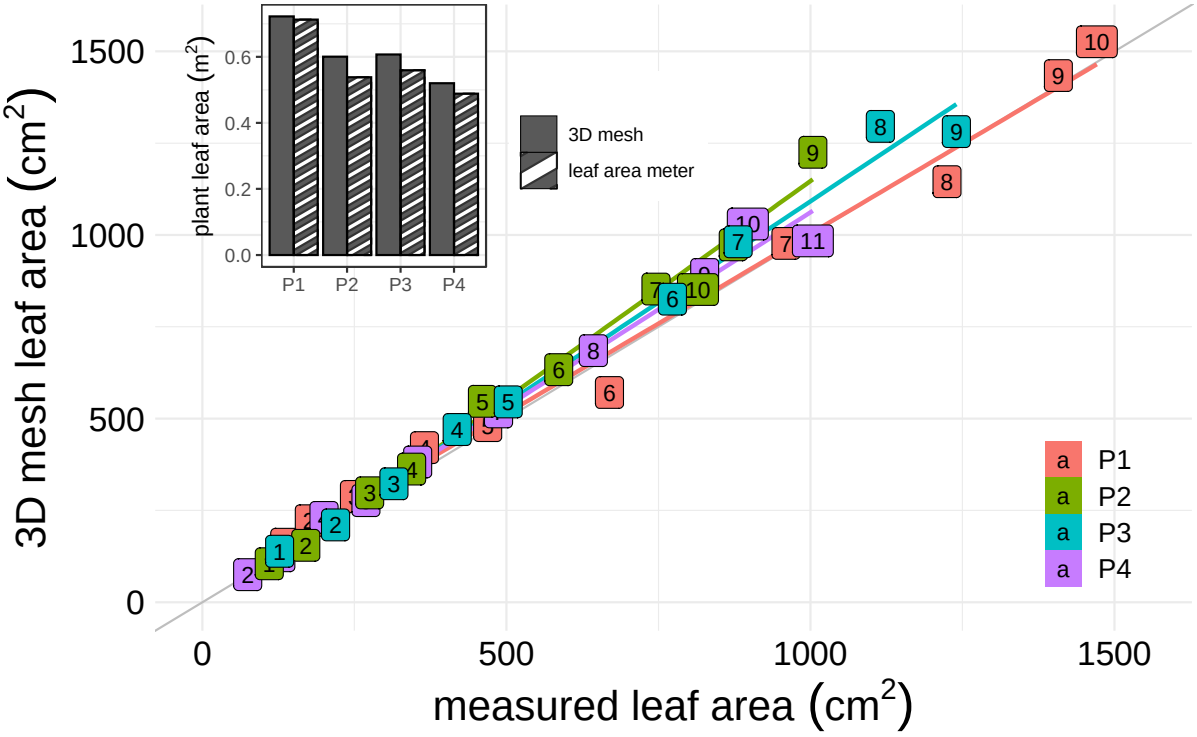

Figure 7: Evaluation of 3D reconstructions based on leaf area. Numbers indicate the leaf number, and colours refer to the plants. The inset represents the total plant leaf area estimated from 3D mesh and measured with the leaf area meter.

Mapping photosynthetically active radiation in the microcosm

We conducted specific measurements to assess the spatial heterogeneity of light within the microcosm using a PAR sensor device (Sunscan, Delta-T, Figure 8). This device is equipped with 60 sensors, each spaced 1.6 cm apart, which allows for a fine-scale mapping of the light environment.

Measurements were performed under three distinct conditions: i) in an empty microcosm to capture both direct and diffuse radiation; ii) in an empty microcosm with black felt applied to the walls to suppress scattered light (Figure 8A); and iii) in the microcosm with a plant present (Figure 8B).

For the empty chamber, light was measured at four vertical heights (21 cm, 51 cm, 81 cm, and 111 cm from the light source) to capture the vertical distribution of radiation. In the presence of a plant, measurements were taken at the top of the pot (105.4 cm from the light source), and at mid-canopy level (91.5 cm from the light source). At each of these heights, we conducted a horizontal mapping by measuring light at eleven positions spanning from 10 cm to 90 cm across the chamber starting from the left side, with additional measurements at 5 cm and 95 cm to capture edge effects. The pot was placed in the centre of the chamber, approximately 56 cm from the lateral and back walls, and a black net was positioned on the chamber floor in all conditions to minimize light reflections. The light source consisted of four LED spots, with its spectral distribution detailed in Supplementary Material Figure S2.

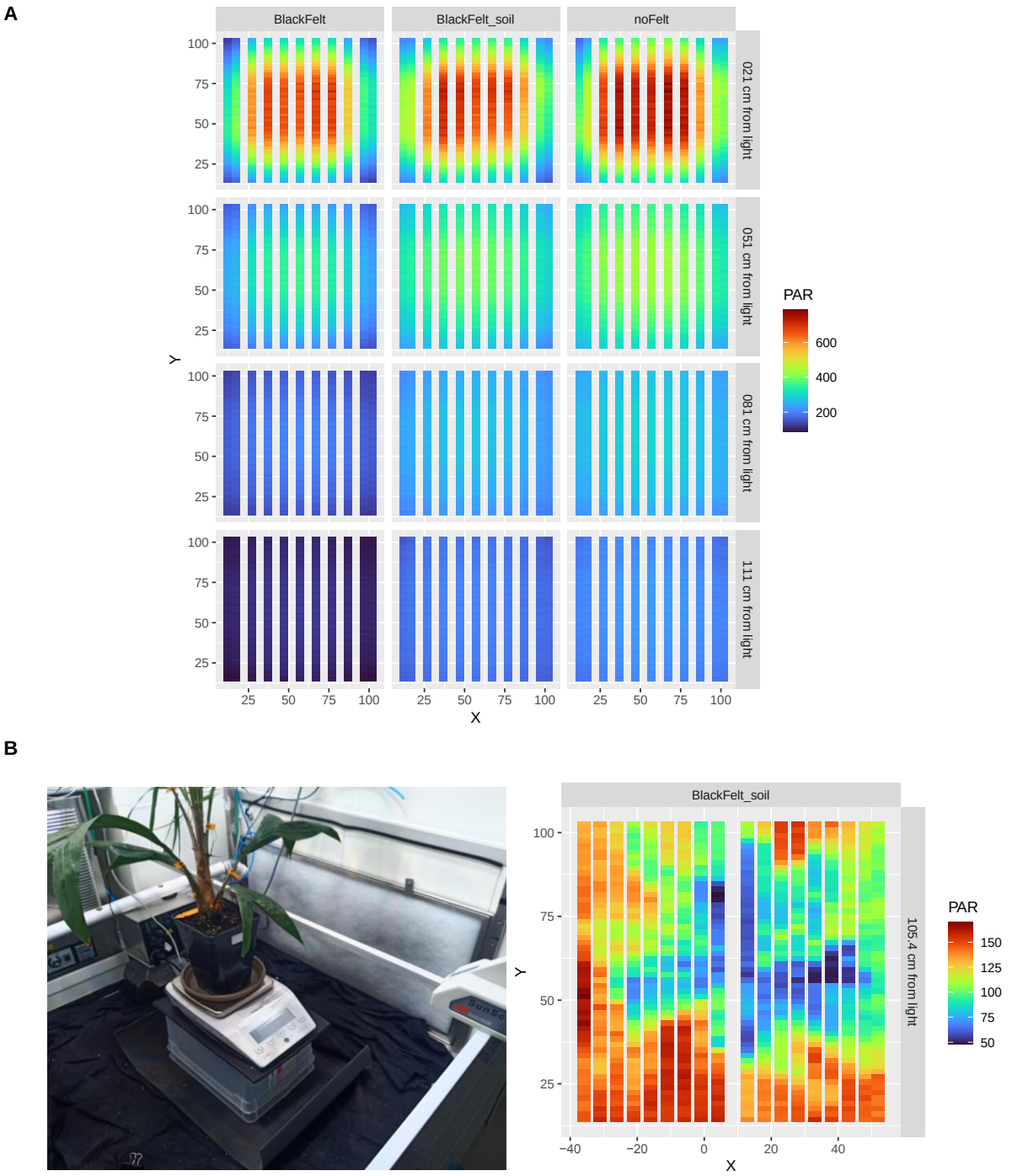

Figure 8: Mapping light distribution within the microcosm using a SunScan (Delta-T) with 60 light sensors. A) Radiation levels vary based on the distance from the light source and the optical properties of the walls and soil (covered or not with black felt to prevent diffusion). B) Monitoring radiation transmission beneath the plant. The colours represent the intensity of photosynthetically active radiation (PAR) in µmol m^{-2} s^{-1}.

Data and code availability

The raw data and scripts used to generate the final database are detailed and accessible on Zenodo (Vezy et al., 2025), the code is also accessible via a Github repository (https://github.com/PalmStudio/Biophysics_database_palm), and we also provide a

companion website (https://palmstudio.github.io/Biophysics_database_palm) showing how computations were made and the main results. The code to trigger the FLIR camera and for logging the precision scale data is also available on dedicated Zenodo repositories (Vezy, 2025a, 2025b).

Author contributions

RP, TA, and RV wrote the manuscript. VT, RP, and RV performed the experiment with the help of SR (portable leaf gas exchange chamber), SD (microcosm functioning and irrigation), CP (CO2 fluxes measurement), DL (light measurements), and MR (lidar measurements and co-registration). RV developed the code to automate transpiration and leaf temperature measurements. RP, RV, TA, and JL worked on the data analysis. JPC helped with funding the study with SMART-RI.

Funding

This research was supported by CIRAD (French Agricultural Research Centre for International Development), an internal call of the AMAP lab “Botany and Modeling of Plant Architecture And Vegetation”, and the PalmStudio research project (SMART-RI and CIRAD project).

References

Blender Online Community, 2022. Blender - a 3D modelling and rendering package.

Busch, F.A., Ainsworth, E.A., Amtmann, A., Cavanagh, A.P., Driever, S.M., Ferguson, J.N., Kromdijk, J., Lawson, T., Leakey, A.D.B., Matthews, J.S.A., Meacham-Hensold, K., Vath, R.L., Vialet-Chabrand, S., Walker, B.J., Papanatsiou, M., 2024. A guide to photosynthetic gas exchange measurements: Fundamental principles, best practice and potential pitfalls. Plant, Cell & Environment 47, 3344–3364. https://doi.org/10.1111/pce.14815

Dreyer, E., Le Roux, X., Montpied, P., Daudet, F.A., Masson, F., 2001. Temperature response of leaf photosynthetic capacity in seedlings from seven temperate tree species. Tree Physiology 21, 223–232. https://doi.org/10.1093/treephys/21.4.223

Duursma, R.A., Medlyn, B.E., 2012. MAESPA: a model to study interactions between water limitation, environmental drivers and vegetation function at tree and stand levels, with an example application to [CO_2] × drought interactions. Geoscientific Model Development 5, 919–940. https://doi.org/10.5194/gmd-5-919-2012

Farquhar, G.D., von Caemmerer, S. von, Berry, J.A., 1980. A biochemical model of photosynthetic CO2 assimilation in leaves of C3 species. Planta 149, 78–90.

Griffon, S., de Coligny, F., 2014. AMAPstudio: An editing and simulation software suite for plants architecture modelling. Ecological Modelling 290, 3–10. https://doi.org/10.1016/j.ecolmodel.2013.10.037

Krinner, G., Viovy, N., de Noblet-Ducoudré, N., Ogée, J., Polcher, J., Friedlingstein, P., Ciais, P., Sitch, S., Prentice, I.C., 2005. A dynamic global vegetation model for studies of the coupled atmosphere-biosphere system. Global Biogeochemical Cycles 19. https://doi.org/10.1029/2003GB002199

Kumarathunge, D.P., Medlyn, B.E., Drake, J.E., Tjoelker, M.G., Aspinwall, M.J., Battaglia, M., Cano, F.J., Carter, K.R., Cavaleri, M.A., Cernusak, L.A., Chambers, J.Q., Crous,

K.Y., De Kauwe, M.G., Dillaway, D.N., Dreyer, E., Ellsworth, D.S., Ghannoum, O., Han, Q., Hikosaka, K., Jensen, A.M., Kelly, J.W.G., Kruger, E.L., Mercado, L.M., Onoda, Y., Reich, P.B., Rogers, A., Slot, M., Smith, N.G., Tarvainen, L., Tissue, D.T., Togashi, H.F., Tribuzy, E.S., Uddling, J., Vårhammar, A., Wallin, G., Warren, J.M., Way, D.A., 2019. Acclimation and adaptation components of the temperature dependence of plant photosynthesis at the global scale. New Phytologist 222, 768–784. https://doi.org/10.1111/nph.15668

Maréchaux, I., Chave, J., 2017. An individual-based forest model to jointly simulate carbon and tree diversity in Amazonia: description and applications. Ecological Monographs 87, 632–664. https://doi.org/10.1002/ecm.1271

Medlyn, B.E., Dreyer, E., Ellsworth, D., Forstreuter, M., Harley, P.C., Kirschbaum, M.U.F., Le Roux, X., Montpied, P., Strassemeyer, J., Walcroft, A., Wang, K., Loustau, D., 2002. Temperature response of parameters of a biochemically based model of photosynthesis. II. A review of experimental data. Plant, Cell & Environment 25, 1167–1179. https://doi.org/10.1046/j.1365-3040.2002.00891.x

Medlyn, B.E., Duursma, R.A., Eamus, D., Ellsworth, D.S., Prentice, I.C., Barton, C.V.M., Crous, K.Y., De Angelis, P., Freeman, M., Wingate, L., 2011. Reconciling the optimal and empirical approaches to modelling stomatal conductance. Global Change Biology 17, 2134–2144. https://doi.org/10.1111/j.1365-2486.2010.02375.x

Schymanski, S.J., Or, D., 2017. Leaf-scale experiments reveal an important omission in the Penman–Monteith equation. Hydrology and Earth System Sciences 21, 685–706. https://doi.org/10.5194/hess-21-685-2017

Vezy, R., 2025a. PalmStudio/FLIR_Vue_Pro-Raspberry_Pi: First release. https://doi.org/10.5281/zenodo.14862498

Vezy, R., 2025b. PalmStudio/Precision_scale-Raspberry_Pi: First stable version. https://doi.org/10.5281/zenodo.14862494

Vezy, R., Perez, R., Torrelli, V., Arsouze, T., 2025. Compiled database, code and raw data for the article “A Comprehensive Database of Leaf Temperature, Water, and CO2 Fluxes in Young Oil Palm Plants Across Diverse Climate Scenarios for the Evaluation of Functional-Structural Models.” https://doi.org/10.5281/zenodo.12705929

Vos, J., Evers, J.B., Buck-Sorlin, G.H., Andrieu, B., Chelle, M., de Visser, P.H.B., 2010. Functional–structural plant modelling: a new versatile tool in crop science. Journal of Experimental Botany 61, 2101–2115. https://doi.org/10.1093/jxb/erp345